JOURNAL OF AIRCRAFT
Vol. 29, No. 3, May–June 1992

Design and Development of a Compressible Dynamic Stall Facility

L. W. Carr*
U.S. Army AVSCOM and NASA Ames Research Center, Moffett Field, California 94035
and
M. S. Chandrasekhara†
Naval Postgraduate School, Monterey, California 93943

A dynamic stall facility offering a unique new capability for studies of compressibility effects on dynamic stall is described. This facility features complete visual access by mounting the test airfoil between optical quality glass windows that are rotated in unison to produce the oscillating airfoil motion associated with helicopter rotor dynamic stall. By using the density gradients associated with the rapidly changing dynamic stall flowfield, this facility permits simultaneous detailed investigation of the flow on the surface as well as in the flowfield surrounding airfoils experiencing dynamic stall.

Nomenclature

c = airfoil chord
f = frequency of oscillation, Hz
k = reduced frequency, $\pi fc/U_\infty = \omega c/2U_\infty$
M_∞ = freestream Mach number
U_∞ = freestream velocity
x = chordwise distance
α = angle of attack
α_a = amplitude of oscillation
α_m = mean angle of attack
ω = circular frequency, radians/s

Introduction

UNSTEADY lift and dynamic stall-delay have been the subject of considerable interest in helicopter and aircraft maneuverability. Prior studies[1,2] have shown that airfoils and wings that are pitched rapidly past the static stall angle can produce lift significantly greater than that obtained in steady flow (for a detailed discussion of the dynamic stall process see Carr[3]). These studies have shown that the dynamic stall process is characterized by a strong vortex that forms on the upper surface of the airfoil, inducing dramatic changes in the lift and moment characteristics of the airfoil (Fig. 1). However, it has also been found that as the freestream Mach number exceeds 0.2, the local flow on the airfoil may reach supersonic velocities (Fig. 2).[2] Figure 3[3] shows that an airfoil that experiences trailing-edge stall for freestream Mach numbers less than 0.2 can experience leading-edge stall as the Mach number increases past 0.2. Thus, compressibility can play a dominant role in altering the flow around the airfoil. In fact, there is experimental evidence that the benefits of dynamic stall may be dramatically attenuated as the freestream Mach number is increased beyond 0.3, as shown in Fig. 4.[3]

One of the major difficulties preventing detailed analysis of the physics of dynamic stall has been the inability to measure the characteristics of this unsteady flow on the surface and in the flowfield simultaneously at conditions representing actual flight. For example, flow visualization of dynamic stall

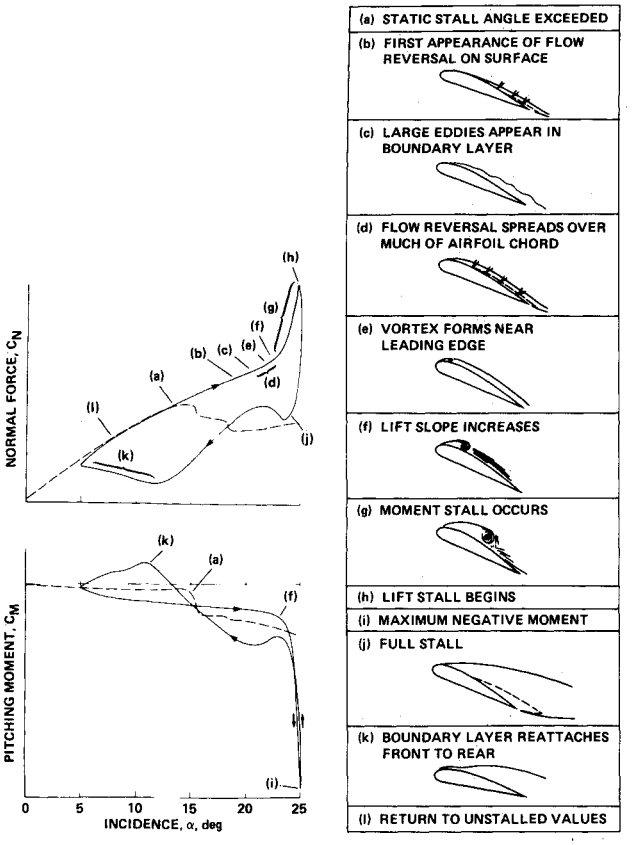

Fig. 1 Lift and moment vs angle of attack for airfoil experiencing dynamic stall.[1]

Presented as Paper 89-0647 at the AIAA 27th Aerospace Sciences Meeting, Reno, NV, Jan. 9–12, 1989; received Jan. 23, 1990; revision received Jan. 8, 1991; accepted for publication Feb. 4, 1991.

*Group Leader, Unsteady Viscous Flows, Fluid Dynamics Research Branch, NASA, and Fluid Mechanics Division, Aeroflightdynamics Directorate, MS 260-1. Member AIAA.

†Adjunct Research Professor and Assistant Director, Department of Aeronautics and Astronautics, U.S. Navy-NASA Joint Institute of Aeronautics. Associate Fellow AIAA.

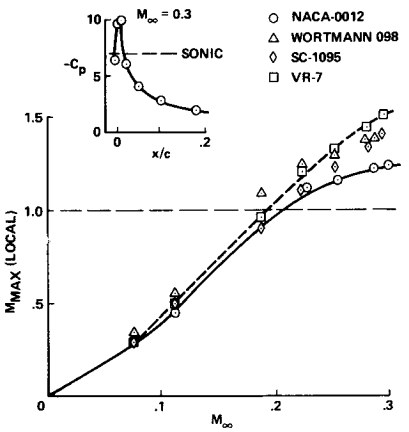

Fig. 2 Local Mach number on leading edge of oscillating airfoil vs freestream Mach number.[2]

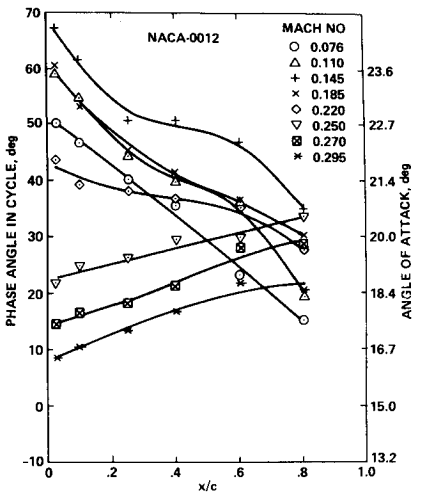

Fig. 3 Location of flow reversal on surface of NACA 0012 airfoil as a function of angle of attack for various Mach numbers for 15° + 10° sin ωt.[2]

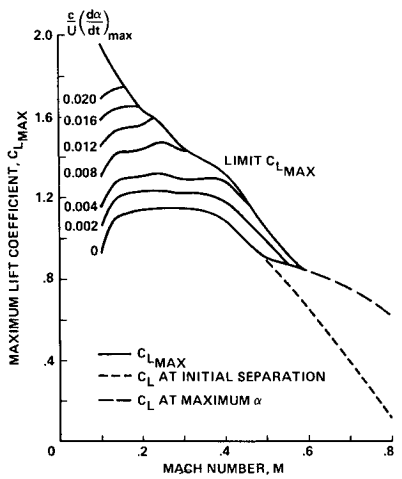

Fig. 4 Effect of maximum pitching rate on lift characteristics of wing model for various Mach numbers.[3]

has been limited to low-speed water or wind tunnels, where hydrogen-bubble or smoke techniques have demonstrated the presence of the dynamic-stall vortex for a wide range of test conditions.[4,5] However, water-tunnel visualization cannot address the question of compressibility effects; smoke-flow visualization becomes very difficult to use in flows there $M_\infty > 0.1$. Smoke becomes highly diffused in rapidly changing flowfields, thus masking many of the important flowfield conditions, and making photography very difficult. It is, therefore, clear that the key to understanding the effect of compressibility on dynamic stall lies in the ability to visualize these complex flow interactions.

Visual study of the flow on oscillating airfoils in compressible flow is made practical by the density gradients inherent in the compressible flow itself. Nonintrusive diagnostic techniques, such as stroboscopic schlieren and holographic interferometry, become viable choices. However, conventional mounting of airfoils between solid tunnel walls severely limits the potential use of these techniques. In those cases where optical quality walls were considered,[6] the massive support structures needed to withstand the large dynamic loads severely blocked major parts of the flow, making visualization of these areas impractical, if not impossible.

These limitations led to the development of the present concept for dynamic-stall testing. The airfoil is pin-mounted between two optical glass windows; these windows are then oscillated simultaneously, permitting completely unobstructed viewing of the complex flow around the airfoil throughout the dynamic-stall cycle.

Design Requirements

The potential for control and use of the beneficial aspects of dynamic stall requires a clear understanding of the flow phenomena that affect the inception and development of the dynamic-stall vortex. Because earlier studies have shown that there is a significant reduction in dynamic-stall overshoot as the Mach number increases past $M_\infty = 0.3$, the present facility has been designed to permit visual study of the flow on oscillating airfoils from $M_\infty = 0.1$ to $M_\infty = 0.5$. The use of optical glass windows with unobstructed view over the airfoil was the primary consideration in the conceptual design of this facility.

The primary occurrence of oscillating airfoil dynamic stall is on helicopter rotors. Experimental research in the helicopter industry has shown that the dynamic stall that appears on full-scale rotors can be documented on small-scale model rotors operated in wind tunnels.[7] Therefore, the present tunnel was designed to incude the flow conditions that appear on typical helicopter model rotors in forward flight (Table 1 presents the conditions that have been run to date). In order to understand fully the changes that occur in the dynamic-stall process as the Mach number varies, the test matrix was designed to bridge the range of conditions from incompressible (for comparison with water-tunnel studies) to strongly compressible $0.3 < M_\infty < 0.5$. The amplitude range was designed to permit 2 deg $< \alpha_a <$ 10 deg variation around mean angles of 0 deg $< \alpha_m <$ 15 deg. This range permits the study of stall-onset delay as well as deep dynamic stall, and also offers the possibility for the study of large-amplitude aeroelastic interactions. The maximum physical frequency chosen for this facility is 100 Hz at maximum oscillation amplitude, thereby representing the conditions of deep dynamic stall at $k = \omega c/2U_\infty = 0.15$ at $M_\infty = 0.5$. It was also specified that the motion of the airfoil be a simple harmonic, e.g., $\alpha = \alpha_m + \alpha_a \sin \omega t$.

Table 1 Experimental conditions

	k						
M	0	0.0125	0.025	0.05	0.075	0.1	0.15
0.15				X		X	X
0.20	X			X	X	X	
0.25	X	X	X	X	X	X	
0.30	X	X	X	X	X	X	
0.35	X	X	X	X			
0.40	X		X	X			
0.45	X		X	X			

Description of Facility

Fluid Mechanics Laboratory

The Compressible Dynamic Stall Facility (CDSF) uses the unique experimental facilities located at the NASA Ames Research Center Fluid Mechanics Laboratory (FML). The laboratory is centered on a multiple in-draft wind-tunnel concept, which permits simultaneous experiments to operate from one drive system. This drive system uses a large evacuation compressor that automatically maintains sufficient vacuum downstream of each test facility to cause sonic velocity to occur in the smallest cross section of each test chamber. This choked-throat concept is used to isolate each test bay and maintain constant flow for a wide range of operating conditions during simultaneous operation of multiple tunnels.

The system is powered by a 113-m^3/s (240,000 cfm), 6.5-MW (9000 hp) centrifugal evacuation compressor. This drive system is fully automated, with control of the compressor directed by an electronic panel that maintains the conditions set by the compressor operator at the start of the test day. Monitoring of the required set pressure and adjustment of the guide vanes and bypass flow is controlled by a computer for efficient compressor operation. The present test constitutes the first experimental program performed in this unique new complex.

Tunnel Design

The CDSF is the test section (35 cm high × 25 cm wide × 100 cm long) of an indraft wind tunnel. The entrance sections of this tunnel have already been used for aeroacoustic studies[8]; the flow uniformity in the tunnel has been reported to be ± 0.25% at 58 m/s, with a turbulence intensity of 0.083% with a bandwidth of 50–50,000 Hz.[9] Because the new test section is dimensionally identical to the above mentioned acoustic wind tunnel (except for circular windows at the sides), no further tests were conducted to establish the flow quality.

The test section is designed to permit continuous variation of mean angle and oscillation amplitude; the mean angle is controlled by angle-of-attack plates that pivot about the center line of the optical glass windows (Fig. 5). Mean angles of 5, 10, and 15 deg can be locked precisely by anchor pins; other mean angles can be established by placing the angle-of-attack plate assembly at the required angle and anchoring the plate through tightening of locking bolts on each side of the tunnel. This angle-of-attack assembly supports the flywheel and motor system so that no change is required in the drive system regardless of the mean angle and/or amplitude chosen. The flywheels serve to store the kinetic energy of rotation through each cycle and keep the speed fluctuations to less than 1%.

The amplitude of oscillation is established by positioning eccentric disks mounted within the flywheels, which in turn are mounted on the angle-of-attack assembly (Figs. 5 and 6). These eccentric disks are keyed to each other within the flywheel shaft, and can be positioned for any half-amplitude value between 2 and 10 deg; the flywheel is marked for accurate selection of the 2-, 5-, and 10-deg-amplitude conditions. The flywheels are connected to the window assemblies through push rods, establishing a four-bar linkage for driving the window/airfoil/window assembly. The system is powered by a 3HP AC motor which is capable of maintaining a constant speed to within 1%.

The airfoil is simply supported between the glass windows by tapered pins located at $x/c = 0.25$ (the axis of rotation for the airfoil and the windows), and $x/c = 0.70$ (Fig. 7). The pins end in spherical tips that are captured by split sleeves, thus ensuring that the dynamic and aerodynamic loads will be transferred to the center of the holes drilled in the windows without inducing any loads due to bending. The pins are inserted into delrin bushings (0.0005 in. thick) to prevent direct metal contact with the glass and to compensate for possible misalignment during assembly of the glass/airfoil/glass system. The delrin sleeves are push-fitted into the glass. It should be noted that this push-fit requirement was the cause of the crack that appears in the schlieren photographs at $x/c = 0.7$. This crack appeared during assembly, and has remained completely stable throughout the range of tests performed in the present study. The damaged window has been replaced, and future photographs will be free of this imperfection.

The windows are 15.2-cm-diam, 2.54-cm-thick, D-shaped schlieren-quality glass (BK-7), supported in magnesium frames that are mounted on bearing races, which permit rotation of the window. A sliding seal is installed to eliminate passage of air into the test section. Detailed mechanical design information can be found in Ref. 10.

Instrumentation

Three high-resolution encoders provide accurate position and frequency information. The mean angle of attack is in-

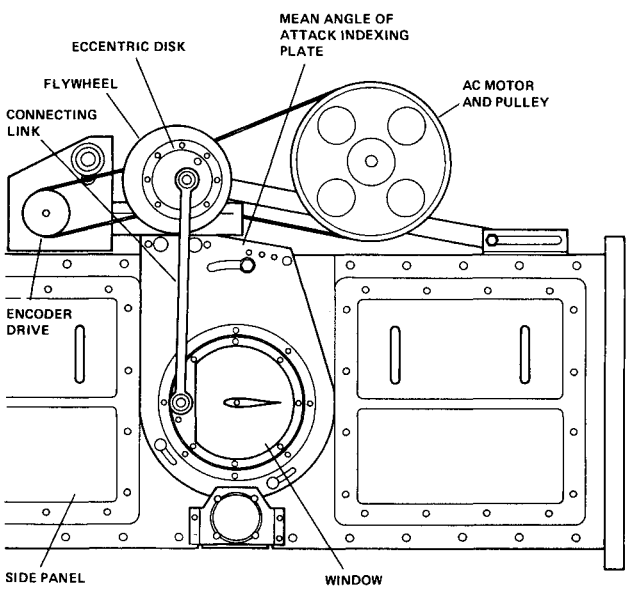

Fig. 5 Side-view of Compressible Dynamic Stall Tunnel test section.

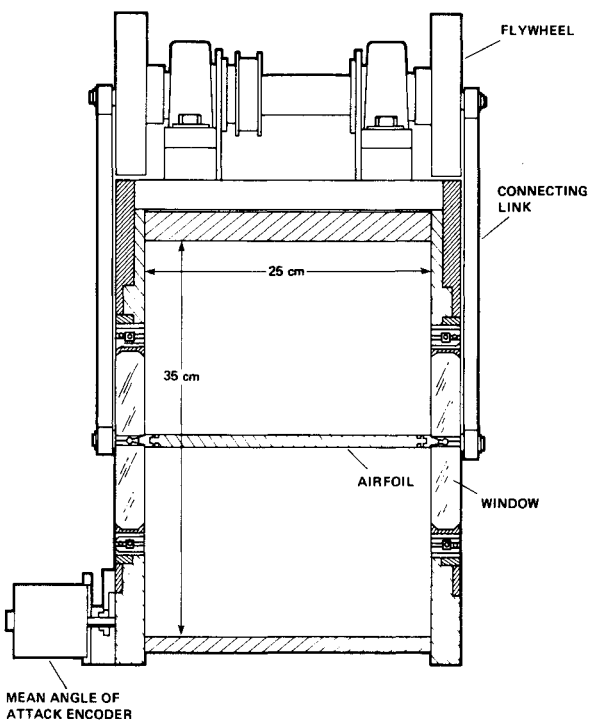

Fig. 6 End-view of test section.

dicated by an absolute position encoder with 3600 counts per revolution (0.1 deg/count). The instantaneous angle of attack is provided by an incremental encoder mounted on the window. The frequency and phase angle are provided by another incremental encoder with 800 counts/cycle of oscillation, and is keyed to the flywheel driveshaft. All encoder outputs are digital and are read into a Microvax II computer, which is used to control the experiment.

The primary instrumentation for this facility is nonintrusive; the instrumentation presently includes a stroboscopic schlieren and a two-component, laser-Doppler velocimeter (LDV). Future systems will include holographic interferometry and laser-sheet visualization. The schlieren system,[9] shown in Fig. 8, consists of a stroboscopic light source that can be triggered either manually or by computer control at any desired point in the cycle; single and repetitive triggering are available. The schlieren system uses two large spherical mirrors (45 cm in diameter with a 3-m focal length) located 3 m from the test section. This offers a very sensitive system because sensitivity is directly proportional to focal length. The image produced by the schlieren system can be recorded using single-frame photographic film, videorecorder, or stop-frame 16-mm movie film.

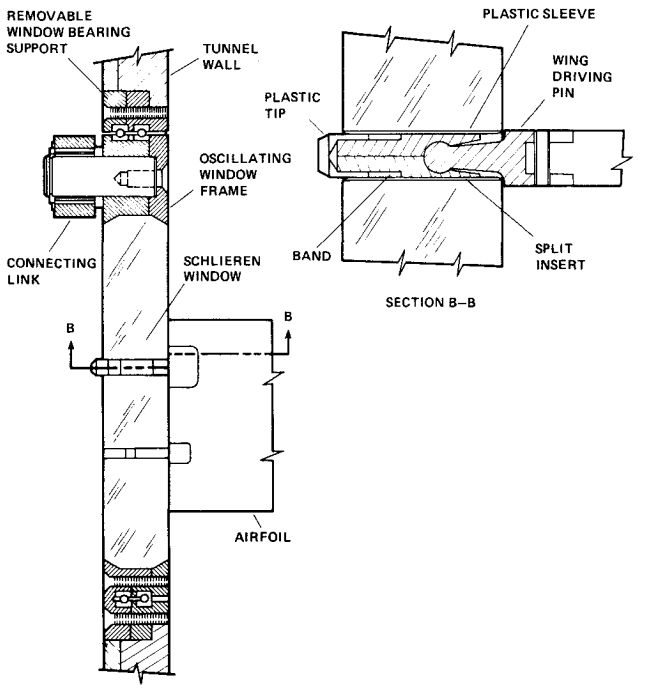

Fig. 7 Detail of airfoil support at window.

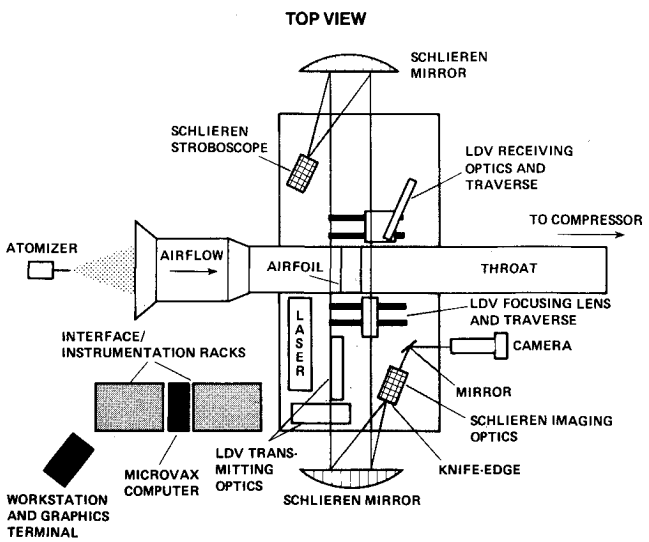

Fig. 8 Schematic of Compressible Dynamic Stall Tunnel schlieren and LDV setup.

The LDV system uses standard optics and counter processors. The data from this system are acquired by the computer in the Direct Memory Access (DMA) mode using an eight-channel multiplexer to check for coincidence of the data on two channels. The encoder data are also input to the multiplexer through a system that records the encoder value only when coincident LDV data are obtained.

Static pressures are obtained at various locations in the tunnel test section, diffuser, and variable throat. These pressures are measured by a scani-valve system that uses a high-resolution pressure transducer, and they are recorded by computer for future reference. Provision has been made for installing instantaneous pressure transducers in the upper and lower tunnel surfaces, so that quantitative dynamic wall effects can be obtained during the oscillating airfoil tests.

Typical tunnel wall static pressure distributions are presented in Fig. 9. In this figure, the range of x/c extends from the beginning of the test section to the end of the variable throat diffuser and $x/c = 0$ corresponds to the trailing edge of the airfoil.

This figure also shows that at $M_\infty = 0.30$, and $f = 5$ Hz, the static pressure in the test section is nearly constant (except for the slight decrease resulting from the growth of the tunnel wall boundary layers). The minimum cross section of the variable throat diffuser is located at $x/c = 11$. The steep rise in static pressure at $x/c = 14$ is due to a shock forming in the diverging section of the diffuser. Similar results were obtained throughout the range of Mach numbers, with or without the airfoil, except that the strength of the shock in the diffuser became weaker with increasing Mach number. At $M_\infty = 0.5$

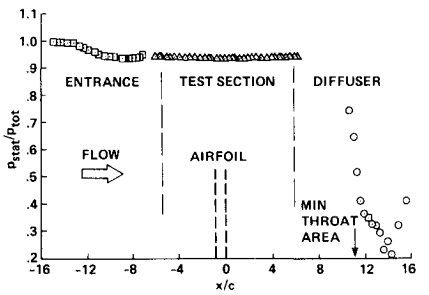

Fig. 9 Tunnel wall static pressure distribution, $M_\infty = 0.3, f = 5$ Hz.

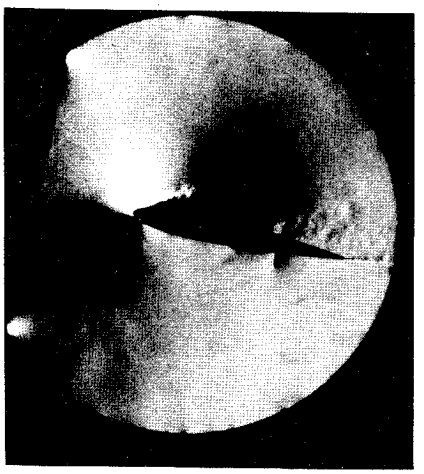

Fig. 10 Photograph of flow on oscillating airfoil during dynamic stall, $M_\infty = 0.30$, $k = 0.025$, $\alpha = 13.8$ deg. (Note that the vertical lines that appear above and below the airfoil at $x/c = 0.7$ are due to a crack in the optical window.)

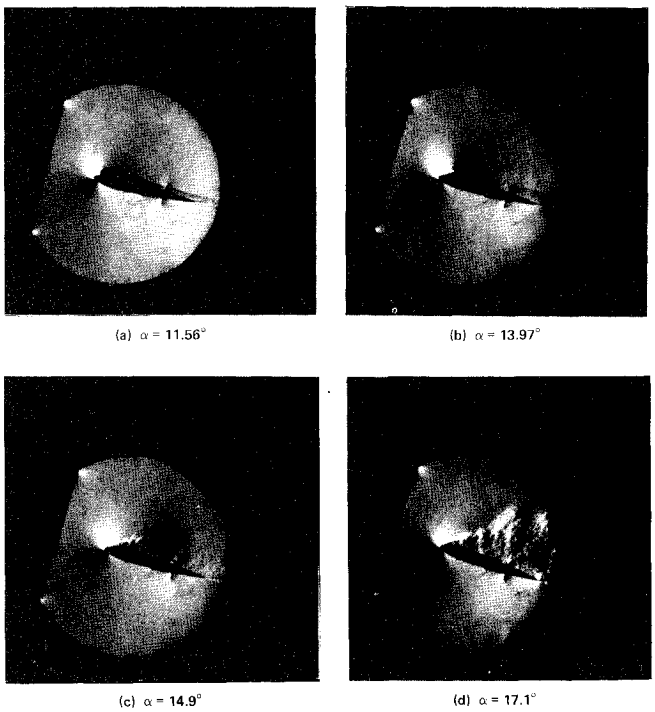

Fig. 11 Dynamic stall at $M_\infty = 0.30$, $k = 0.05$: a) prestall; b) vortex formation; c) vortex moving down airfoil; d) vortex leaves trailing edge.

the pressure distribution indicated a marginally choked diffuser flow; therefore, the upper limit on the Mach number for the present study was set at 0.45 (a higher Mach number can be obtained by setting a lower set-point for the compressor, or by modifying the inlet/contraction section of the wind tunnel).

Results of Schlieren Study

The stroboscopic schlieren technique has been fully exercised in the study of the formation and development of the dynamic-stall vortex on oscillating airfoils for a variety of test conditions (for details see Ref. 11). As is well known, the schlieren technique is based on the fact that light beams are deflected by changes in density gradient in the airflow. This effect is dramatically demonstrated in Fig. 10, which shows the presence of the dynamic-stall vortex at 50% chord of an oscillating airfoil at $M_\infty = 0.3$, $k = 0.025$ (note that the vortex is clearly defined even though the reduced frequency is low).

Figure 11 presents photographs of the development of this stall process at various phase angles during the cycle at $M_\infty = 0.3$, $k = 0.05$. The strength of the vortex is such that it can be detected in flows as low as $M_\infty = 0.15$ without enhancement. It should be noted that these images are the first visualizations of this unsteady flow that are accurate representations of the instantaneous vortex strength because the density gradients, which cause the schlieren image to appear, are occurring at the instant the photograph is taken. In contrast, the particle path lines that are the source of smoke-flow or hydrogen-bubble visualization present only an image of what the vortex has done to the flow up to the time of the photograph, and, thus, give a limited indication of the strength of the vortex at the time the photograph was taken.

Concluding Remarks

A dynamic-stall facility has been developed that offers a unique capability for studying the effects of compressibility on dynamic stall. Complete optical access is assured by mounting the test airfoil between optical-glass windows, which are then oscillated in unison to produce the unsteady motion characteristic of helicopter rotor airfoils in forward flight. Utilizing the density gradients that occur in the flowfield around oscillating airfoils even at moderate freestream Mach numbers, this facility permits a detailed investigation of the events on the surface to be simultaneously coupled to the flowfield surrounding airfoils that are experiencing dynamic stall. Schlieren studies of oscillating airfoils across a wide range of Mach numbers and frequencies have been performed, and the resultant flow visualization offers the first truly instantaneous visualization of the unsteady flow associated with the dynamic-stall phenomenon.

Acknowledgments

We acknowledge the invaluable contributions of the late Satya Bodapati, who was instrumental in developing the technique presented in this paper. This work was performed under ARO MIPR-ARO-137-86, and AFOSR-MIPR-88-0010 to the Naval Postgraduate School, with additional funding support from the Naval Air Systems Command and the Naval Postgraduate School. The design support of C. D. Sticht and the technical support of M. J. Fidrich throughout the course of this project is greatly appreciated.

References

[1]Carr, L. W., McAlister, K. W., and McCroskey, W. J., "Analysis of the Development of Dynamic Stall Based on Oscillating Airfoil Experiments," NASA TN-8382, Jan. 1977.

[2]McCroskey, W. J., McAlister, K. W., Carr, L. W., Pucci, S. L., Lambert, O., and Indergand, R. F., "Dynamic Stall on Advanced Airfoil Sections," *Journal of American Helicopter Society*, July 1981, pp. 40–50.

[3]Carr, L. W., "Progress in Analysis and Prediction of Dynamic Stall," *Journal of Aircraft*, Vol. 25, No. 1, 1988, pp. 6–17.

[4]McAlister, K. W., and Carr, L. W., "Water-Tunnel Visualization of Dynamic Stall," *Journal of Fluids Engineering*, Vol. 101, No. 3, 1979, pp. 376–380.

[5]Helin, H. E., Robinson, M. C., and Luttges, M. W., "Visualization of Dynamic Stall Controlled by Large Amplitude Pitching Motions," AIAA Paper 86-2281-CP, Aug. 1986.

[6]Lee, G., Buell, D. A., and Licursi, J. P., "Laser Holographic Interferometry for an Unsteady Airfoil Undergoing Dynamic Stall," *AIAA Journal*, Vol. 22, No. 4, 1984, pp. 504–511.

[7]McCroskey, W. J., and Fisher, R. K., "Detailed Aerodynamic Measurements on a Model Rotor in the Blade Stall Regime," *Journal of the American Helicopter Society*, Vol. 17, No. 1, Jan. 1972, pp. 20–30.

[8]Davis, S. S., "Measurement of Discrete Vortex Noise in a Closed-Throat Wind Tunnel," AIAA Paper 75-488, March 1975.

[9]Kadlec, R. A., and Davis, S. S., "Visualization of Quasiperiodic Flows," AIAA Paper 78-502R; see also *AIAA Journal*, Vol. 17, No. 11, 1979, pp. 1164–1169.

[10]Sticht, C. D., "Development of Drive Mechanism for an Oscillating Airfoil," Symposium on Aerospace Mechanisms, NASA Langley Research Center, Hampton, VA, May 4–6, 1988.

[11]Chandrasekhara, M. S., and Carr, L. W., "Flow Visualization Studies of the Effect of Mach Number on Dynamic Stall," *Journal of Aircraft*, Vol. 27, No. 3, 1990, pp. 516–522.